

Poly(vinyl Chloride) and Wood Flour Press Mould Composites: New Bonding Strategies

Nuno Rocha,^{1,2} Jorge F.J. Coelho,¹ Ana C. Fonseca,¹ Algy Kazlauciusas,² Maria H. Gil,¹ Pedro M. Gonçalves,³ James T. Guthrie²

¹CIEPQPF, Chemical Engineering Department, University of Coimbra, Coimbra 3030-790, Portugal

²Department of Colour Science, University of Leeds, Leeds LS2 9JT, United Kingdom

³Cires S.A. – Companhia Industrial de Resinas Sintéticas, Apartado 20, Estarreja 3864-752, Portugal

Received 19 September 2008; accepted 15 March 2009

DOI 10.1002/app.30419

Published online 29 April 2009 in Wiley InterScience (www.interscience.wiley.com).

ABSTRACT: In this work, different strategies for improving the association between hydrophilic wood flour surfaces and poly(vinyl chloride) (PVC) hydrophobic surfaces were tested. Three new coupling agents, based on living radical polymerisation (LRP), involving PVC were synthesised and tested in formulations with PVC and wood flour. The melt mixing behaviour was analysed in terms of the torque exerted by the mixing blades and related to the structural properties of the mixture. These products were ground and sheets were produced by press moulding. The composites were characterised by dynamic

mechanical analysis. It was found that the use of a new block copolymer poly(vinyl chloride)-*b*-poly(hydroxypropyl acrylate)-*b*-poly(vinyl chloride), prepared by LRP, increases the elastic modulus of the composite, under controlled conditions, involving the use of specific amounts of the copolymer. © 2009 Wiley Periodicals, Inc. *J Appl Polym Sci* 113: 2727–2738, 2009

Key words: poly(vinyl chloride) (PVC); composites; living polymerisation; rheology; thermal properties

INTRODUCTION

Poly(vinyl chloride) (PVC)/wood flour composites are the subject of considerable research. These materials are used in various applications such as window/door profiles, decking, railings, and sidings. Wood flour polymer composites can have a longer life than native wood, as they are less susceptible to moisture-induced swelling, shrinking, and biodeterioration. Wood plastic composites (WPC) take advantage of the beneficial properties of both the wood and the plastic components.^{1–6}

The main disadvantage with most composites of this type is the weak interfacial adhesion that arises between the two components. A possible solution is to use compatibilisers, such as block copolymers and coupling agents. The inclusion of the most common materials provides increasing hydrophobicity in the wood flour phase, due to chemical reaction of each specific group with the hydroxyl groups of the wood. The surface tension of wood flour is reduced and approaches that of the molten thermoplastic. The most common coupling agents are organic acids, anhydrides, isocyanates, and silanes.^{7–12}

The use of silane-based coupling agents offers one of the more successful routes to improving the association between fibres and polymers. These can act as a bridge between the hydrophilic regions and the hydrophobic regions of the materials. Acids and bases catalyse the hydrolysis of the alkoxy silane to the corresponding silanol, which can later undergo condensation reactions. However, the formation of polysiloxanes, inhibits the adsorption of the silane beyond the fibre surface, so that in highly concentrated silane solutions, there is no additional silane adsorption. After hydrolysis, the silanols slowly condense to form oligomeric species.^{13–19}

The conventional free-radical polymerisation of vinyl chloride is the only industrial process that is used for the synthesis of PVC. Living radical polymerisation (LRP) provides an efficient tool for polymer synthesis, yielding macromolecules with controlled molecular weights and narrow polydispersities. The macromolecules are also free of structural defects and contain long-lived chains that can be further activated. The LRP of VC, initiated with CHI₃ and catalysed by Na₂S₂O₄, is mediated mainly by a combination of competitive single electron transfer (SET) and degenerative chain transfer (DT) and provides a novel pathway to living radical polymerisation. This reaction can take place in an aqueous medium at room temperature. This polymerisation process is technologically important

Correspondence to: N. Rocha (ccdnmmpr@leeds.ac.uk).

because it requires only common industrial facilities to produce PVC materials that possess the properties described above.^{20–24}

The chloriodomethyl chain ends, arising from the LRP-PVC, can be replaced with other reactive groups, acting as a macroinitiator. The functionalisation of the chain ends is accessible by SET-mediated organic reactions. This method provides the first example of telechelic α - β -di(hydroxy)PVC.²³

Copolymers have been added to improve the mechanical properties of WPC. This improvement is due to a better dispersion of fibres in the matrix, a more effective wetting of the fibres in the polymeric matrix and better association between the two phases. The grafting of the wood also presents a promising approach to the modification of these materials, by the inclusion of hydrophobic groups into the wood flour surface.^{25–27}

The ability to synthesise block copolymers of PVC with acrylates, using the single-electron-transfer/degenerative-chain-transfer LRP (SET-DTLRP) technique is extremely important because, by this method, it is possible to control the influence of the polymers with their different nature on the PVC properties.^{28–31}

Hydroxyl groups can be incorporated in a controlled way into the PVC, by creating a block copolymer of PVC with poly(hydroxypropyl acrylate) (PHPA).³² A new pathway in WPC is thus created since the interaction is increased by modification of the plastic phase, increasing its hydrophilicity. This opens up the possibility for the PVC to bond with the wood flour by hydrogen bonding, or crosslinking, thereby decreasing the degree of wood flour self-entanglement. In the case of PVC-b-PHPA-b-PVC, the copolymer would be expected to interact with the PVC, via the PVC segments, and with the wood flour, via the hydroxyl groups.

This study was aimed at the synthesis of new coupling agents for WPC, based on LRPPVC, to enable coupling between the PVC and the wood flour that displayed strong intermolecular forces via hydrogen and covalent bonding. The materials obtained were characterised by melt mixing torque rheometry and by dynamical mechanical thermal analysis.

EXPERIMENTAL

Materials

Wood flour (WF) from Bubinga (*Swietenia macrophylla*) was donated by DPM - Distribuição e Produção de Móveis (Portugal). These fibres were ground in a cutting mill, Retsch GmbH SM1, with a 500 μ m stainless steel trapezium shaped sieve.

PVC (a suspension grade, with a molecular weight of about 63,000 g mol⁻¹, $K_{\text{value}} = 65.88$, and $d_{50} =$

168.2 μ m) was supplied by Cires, SA (Estarreja, Portugal).

Stabilox CZ 2973 GN (calcium and zinc based soap stabilizer and lubricant), sodium stearate (lubricant), epoxydised soya bean oil (co-stabiliser and internal lubricant in PVC formulation), Kane Ace PA210 (acrylic copolymer (MD-P210-C210) impact modifier and lubricant), and wax PE520 (KWPEI 15) (lubricant for plastics) were provided by Cires.

Hydroxypropyl acrylate (HPA) (95%), dimethyl sulfoxide (99+%), trimethoxyvinylsilane (97%), sodium dithionite (85%) ($\text{Na}_2\text{S}_2\text{O}_4$), sodium bicarbonate (99+%) (NaHCO_3), 2-allyloxyethanol (98%), and iodoform (99%) (CHI_3) were purchased from Sigma-Aldrich (Portugal).

Isopropanol, hydrochloric acid (37% w/w), ethanol and methanol were purchased from José M. Vaz Pereira, S.A. (Portugal). Hydroxypropyl methyl cellulose (Methocel F50) and partially hydrolysed poly(vinyl alcohol) (PVA) were provided by Cires, S.A (Portugal). Vinyl chloride was purchased from ShinEtsu (Japan).

Coupling agents

LRP-PVC preparation

The LRP-PVC synthesis was carried out in a 5L pilot reactor charged with 3.00 L of water, 128.84 g of a 3% aqueous solution of PVA, and 89.06 g of a 1.86% aqueous solution of methocel MF50. The other compounds were then weighed and charged into the reactor: 9.24 g of CHI_3 , 32.70 g of catalyst $\text{Na}_2\text{S}_2\text{O}_4$, 7.89 g of buffer NaHCO_3 , and 1.00 L of vinyl chloride monomer (VCM). The reactor was closed and sealed. The oxygen was removed from the reactor by applying four cycles of vacuum and nitrogen. The VCM (1.00 L) was charged and the reactor was heated up to the polymerisation temperature (42°C). The reaction time was 24 h. The product was rinsed three times with water and then filtered. The LRP-PVC was dried in an oven at 70°C.

Wood flour-PVC covalent bonding (PVC-WF)

A solution containing 225 mL of trimethoxyvinylsilane, 50 mL of distilled water, 240 mL of isopropanol, and 3 mL of chloridric acid was prepared. 8.5 grams of Bubinga wood flour were poured into the prepared solution. The contents were left in a 1-L Parr Instrument Co. 4523 Pressure Reactor for 5 h at 30°C, with an agitation of 200 rpm and with an absolute pressure of 3 bar. The fibres were washed 5 times with distilled water using a vacuum filtration unit. The modified fibres (WFmod) were dried at room under vacuum for 4 days at 70°C.

TABLE I
Composition of Each Mixture (% w/w)

Component	M00	M01	M02	M03	M04	M05
PVC	100.0	80.0	70.0	70.0	76.5	76.5
WF		20.0	20.0	20.0	20.0	20.0
PVC-OH			10			
PVC-PHPA				10	3.5	
PVC-WF						3.5

A 1-L Parr Instrument Co. 4523 Pressure Reactor was charged with 400 mL of dimethyl sulfoxide, 4.400 g of LRP-PVC [Mn (TriSEC) = 41,196 g mol⁻¹], 41.7 mg of sodium dithionite, 14.8 mg of sodium bicarbonate (99+%) and 1.500 g of WFmod. The reactor was conditioned with nitrogen for 10 min. Then the inlet and outlet nitrogen valves were closed until the system reached a constant pressure of 2.5 bar. The reaction mixture was stirred at 200 rpm at 70°C. After 4 h, the reactor was emptied and the mixture was poured into 3 L of ethanol. The product was filtered and rinsed three times with methanol and dried in a vacuum oven at 70°C.

LRP-PVC functionalisation (PVC-OH)

A 1-L Parr Instrument Co. 4523 Pressure Reactor was charged with 600 mL of dimethyl sulfoxide, 6.600 g of LRP-PVC [Mn (TriSEC) = 41,196 g mol⁻¹], 1.400 g of Na₂S₂O₄, 1.400 g of NaHCO₃ and 24 mL of 2-allyloxyethanol. The reactor operation and product purification were undertaken in the same way as previously outlined in Section 2.2.1.

PVC-b-PHPA-b-PVC synthesis (PVC-PHPA)

The α,ω -diiodopoly(HPA) synthesis was carried out in a 5 L pilot reactor by the SET-DTLRP route, initiated with 5.32 g of CHI₃ in 1.2L deionised water at 25°C. The reactor was also charged with 0.40 L of HPA, 9.42 g of catalyst Na₂S₂O₄, 4.54 g of buffer NaHCO₃, 45.99 g of a 3% aqueous solution of PVA, and 31.79 g of a 1.86% aqueous solution of methocel F50. The reaction was undertaken during 6 h at a polymerisation temperature of 42°C. A sample of the macroinitiator PHPA was collected at the end of this first stage.

Afterwards, the reactor was charged with 1.5 L of water, 96.59 g of a 3% aqueous solution of PVA, 66.67 g of a 1.86% aqueous solution of MF50, 18.84 g of a catalyst, Na₂S₂O₄, 1.65 g of the buffer NaHCO₃, and 0.75 L of vinyl chloride monomer (VCM). The reactor was heated up to the polymerisation temperature (42°C) and the reaction was undertaken during 24 h. This last stage makes possible the completion of the synthesis of the copolymer PVC-b-PHPA-b-PVC (PVC-PHPA).

Before each of the two reactions, the reactor was closed and flushed 5 times with nitrogen for 5 min. A vacuum was applied until 0.10 bar for 5 min. The

product was rinsed 3 times filtered with water and dialysed in water. Finally, the block copolymer was dried in a vacuum oven at 70°C.

Processing

Preparation of PVC – rigid formulation

PVC and the additives needed to create a rigid standard formulation were mixed in a high-speed mixer. The solid components were poured into the mixer and mixed for 1 min at 1000 rpm. Then the speed was increased to 2500 rpm. This led to a temperature increase and when it reached 70°C, the speed was decreased to 1000 rpm and the liquid components were added. Then the speed was increased again to 2000 rpm. Finally, when the temperature reached 110°C, the cooling water was turned on and the speed reduced to 1200 rpm. The mixture was collected when the stock temperature was about 50°C.

The PVC rigid formulation was prepared with 100 phr (per hundred of PVC) of PVC, 4 phr of Stabilox CZ 2973 GN, 3 phr of epoxydised soya bean oil, 0.5 phr of sodium stearate, 1 phr of PA210, and 0.5 phr of PE520.

PVC, Bubinga wood flour and coupling agents blending

The composites were compounded using a Plastograph Brabender mixer W50EHT, with two rotors. The mixing temperature was set to 200°C. The mixture was collected after it reached the melting point, to avoid degradation. The fusion chamber was loaded with 40 grams of raw-materials and the mixing speed set to 40 rpm. Table I gives the composition of each sample.

Press mould composites

The fused and mixed materials, obtained in a solid form were then ground in a Retsch GmbH SM1 cutting mill, fitted with a 500 μ m stainless steel trapezium shaped sieve.

The obtained ground materials were then used to manufacture the desired boards by press moulding in a laboratory hydraulic hot press (412BCE, Carver). The materials were pressed for 2 min at 4 metric tons, to reach the plates' temperature (190°C). They were then pressed for 3 min at 11 metric tons. Afterwards, cooling was applied with pressurised air until a temperature below 100°C was reached.

Characterisation techniques

Dynamic mechanical thermal analysis

Dynamical Mechanical Thermal Analysis (DMA) of 2 mm thick specimens, of a size 6.5 mm \times 6.0 mm,

was performed using a Triton Tritec 2000 unit in single cantilever bending, in the multifrequency mode (1 Hz, 3 Hz, 5 Hz, and 10 Hz), with a standard heating rate of $2^{\circ}\text{C min}^{-1}$. The composites were previously moulded with the required dimensions, following the procedure given in Section 2.3.3. The powders were characterised in the Constrain Layer Damping mode, with a standard heating rate of $2^{\circ}\text{C min}^{-1}$, at the same frequencies as those indicated above. The glass transition temperature (T_g) was determined as the peak in $\tan \delta$ (E''/E'). Here, E'' and E' are the loss modulus and storage modulus values, respectively. Each run was repeated twice to establish the reproducibility of the results. The results presented correspond to the average value.

Thermogravimetric analysis

Thermogravimetric Analysis (TGA) was used to determine the thermal behaviour of the raw-materials and of the composites under non-isothermal conditions. The measurements were carried out using a TA Instruments SDT Q600 unit (thermogravimetric sensitivity: $0.1 \mu\text{g}$). Alumina crucibles were employed. The calibration was performed in the range from 25°C to 1000°C with tin and lead as the standards. Samples were loaded into open alumina crucibles. A dry nitrogen purge flow of 100 mL min^{-1} was used in all measurements. Sample weights ranging from 5 to 10 mg were used.

Nuclear magnetic resonance (NMR)

The ^1H -NMR spectra (500 MHz) were recorded on a Bruker DRX 500 spectrophotometer at 32°C in THF-d_8 . ^{13}C NMR spectra of the solid samples were obtained in a 9.4 T Bruker Avance 400 WB spectrophotometer (DSX model) on a 4 mm double-bearing probe, at 100.6 MHz. The solid state NMR experiments were conducted at room temperature under a CPMAS frequency of 9000 Hz.

Fourier transform infrared spectroscopy

Fourier Transform Infrared Spectra (FTIR) were obtained using a Nicolet 750 unit, with a Golden Gate ATR accessory (Specac). The products were analysed as prepared. The resolution was 4 and the number of scans was 64.

Size exclusion chromatography

The chromatography parameters of the samples were determined using a HPSEC unit (High Performance Size Exclusion Chromatography); Viscotek (Dual detector 270, Viscotek, Houston) with differential viscometry (DV); right-angle laser light scatter-

ing (RALLS, Viscotek) and RI (Knauer K-2301) detection. The column set consisted of a PL 10- μm guard column ($50 \times 7.5 \text{ mm}^2$) followed by two MIXED-B PL columns ($300 \times 7.5 \text{ mm}^2$, $10 \mu\text{m}$). The HPLC pump (Knauer K-1001) was set with a flow rate of 1 mL/min . The eluent (THF) was previously filtered through a $0.2 \mu\text{m}$ filter. The system was also equipped with a Knauer online degasser. The tests were done at 30°C using an Elder CH-150 heater. Before injection ($100 \mu\text{L}$), the samples were filtered through a PTFE membrane with $0.2 \mu\text{m}$ pores. The system was calibrated with narrow molar mass poly(styrene) standards.

Chlorine microanalysis

The determination of the chlorine content was performed by Schoniger flask combustion and titration with mercury nitrate. The sample (placed in platinum basket) was combusted in a hermetically sealed Schoniger flask, previously filled with oxygen and allowed to stand for 20 to 30 min. Following this time period, the basket was placed in the flask and washed with the minimum amount of water. Bromophenol blue and nitric acid solution were added dropwise until yellow colour was achieved. Then 0.5 mL more of nitric acid, 50 mL of ethanol, and diphenyl carbazone indicator were added. Titration to a purple end point was undertaken with the 0.05 M mercuric nitrate solution. A standard determination was carried out on a standard of known percentage of chlorine (p-chlorobenzoic acid).

Flexural experiments

The flexural tests were performed using a DARTEC Universal Testing unit with a servo-hydraulic function of 200 kN capacity, fitted with a 5 kN loadcell calibration, including increments of 0.001%. These tests were performed according to the ASTM D790-03 (procedure A), with five specimens for each sample being tested (2.0 mm in thickness, 55 mm in length, and 12.7 mm in width), a crosshead motion rate of 1.2 mm/min , until a midspan deflection of 6 mm and a support span of 38 mm were achieved.

Scanning electron microscopy

The morphology of the materials was investigated using a JEOL JSM-820 scanning electron microscope (SEM). All of the specimens were coated with gold using a Bio-Rad SC500 diode sputter coating unit. The samples were examined over the magnification range from $\times 20$ to $\times 1000$ using an accelerating voltage of 5 kV.

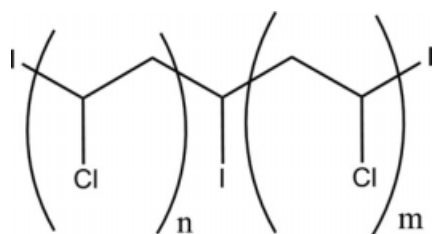


Figure 1 Chemical structure of LRP-PVC²¹.

RESULTS AND DISCUSSION

Coupling agents synthesis

The synthesis of PVC-WF and PVC-OH depended on the synthesis of LRP-PVC. This polymer was synthesised through a mechanism that was developed in previous work.²¹ The proposed chemical structure is shown in Figure 1.

The LRP-PVC was analysed by ¹H-NMR, revealing the presence of terminal active chains ends (-CHClI) between 6.1 and 6.3 ppm and the absence of any structural defects (Fig. 2) as described previously.³² SEC analysis revealed a numerical molecular weight of 42,000 g/mol with a polydispersivity of 2.831.

PVC-WF

During the first stage, the presence of water, chloridric acid, and isopropanol allows the hydroxyl groups (present in the cellulose of the wood) to react with the trimethoxyvinylsilane through partial hydrolysis and co-condensation,¹⁷ making it possible to synthesise WFmod. A possible chemical structure for WFmod is shown in Figure 3.

The presence of the vinyl groups in WFmod allows functionalisation of LRP-PVC, by a mecha-

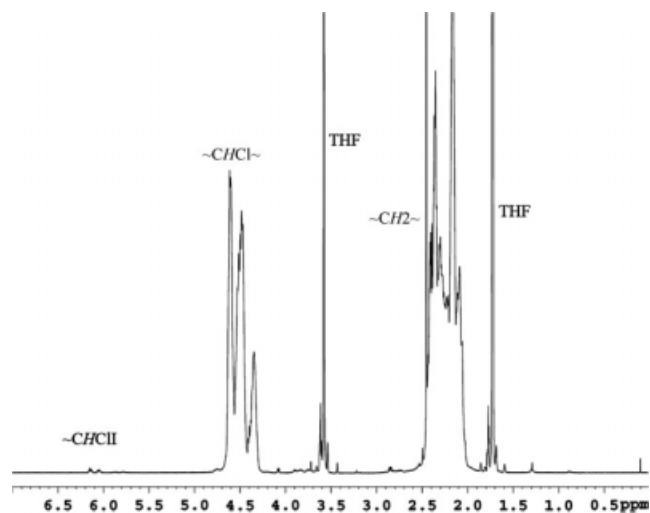


Figure 2 500 MHz ¹H-NMR of the α,ω -diiodo(PVC) prepared by SET-DTLRP.

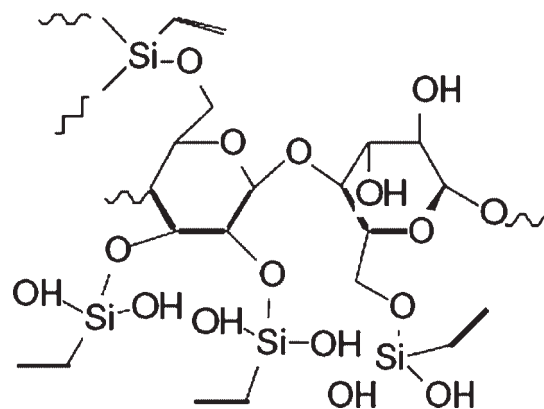


Figure 3 Chemical structure of WFmod.

nism described in previous work.²³ The double bonds of WFmod react at the edges of the LRP-PVC through the iodine groups, resulting in a PVC-WF, with the chemical structure shown in Figure 4.

Figure 5 represents the FTIR analysis of Bubinga wood flour (WF), the Bubinga wood flour modified with trimethoxyvinylsilane (WFmod), and the product of reaction between WFmod and LRP-PVC (PVC-WF). The WFmod trace shows that the vinyl groups were present in the sample. The PVC-WF spectra shows that significant proportion of the vinyl groups reacted with the LRP-PVC, as observed from the decrease in the appropriate FTIR band. The broad band between 1100 and 1000 cm^{-1} and the bands between 1000 and 950 cm^{-1} are due to the presence of the -Si-O-Si- and -Si-O-CH₂-bonds³² respectively. Thus, Figure 5 shows the presence of these groups in WFmod and PVC-WF. This band is less pronounced in the spectrum of PVC-WF than in WFmod, indicating that the reaction with LRP-PVC has broken much of the associations between the silane groups. The peak at 600 cm^{-1} indicates the presence of C-Cl bonds which supports the presence of PVC in the final structure.

PVC-OH

This telechelic material was functionalised following the procedure described in Section 2.2.3 for which the mechanism is described in previous work.²³ Figure 6, shows the chemical structure of PVC-OH.

Figure 7 shows the FTIR spectra for the functionalised PVC and the comparison spectra of the raw-

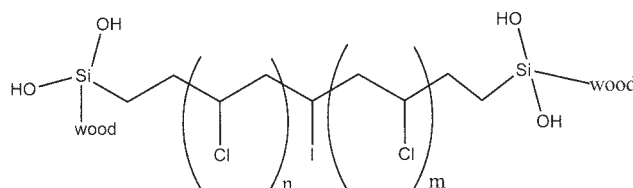


Figure 4 Chemical structure of PVC-WF.

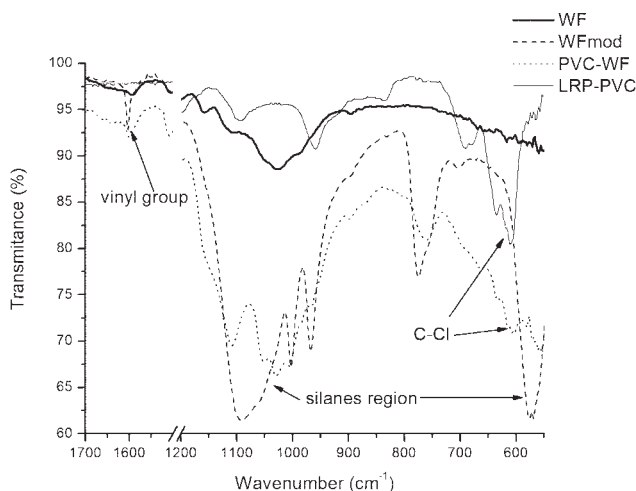


Figure 5 FTIR spectra of WF, WFmod, PVC-WF, and LRP-PVC (vinyl, silane, and C-Cl regions).

materials. Hydroxyl groups were incorporated into the PVC, as suggested by the presence of the broad band for hydroxyl group as a small band between 3600 and 3200 cm^{-1} . Since the proportion of 2-allyloxyethanol is very small compared with that of the LRP-PVC, it is not surprising to see that there is only a small peak for the hydroxyl band in the FTIR spectrum of PVC-OH. Note also, that the vinyl group band at 1600 cm^{-1} , of 2-allyloxyethanol, is not present for PVC-OH, suggesting that there is no residual monomer present.

PVC-PHPA

As described in previous work,²⁹ PVC-PHPA synthesis by the SET-DTLRP approach is achieved by synthesising as the first stage the acrylate polymer, in this case poly(hydroxypropyl acrylate). In a second stage, polymerisation of VCM on the acrylate polymer chain edges is brought about. The resulting structure is represented in Figure 8.

Figure 9 shows the FTIR spectra for sample of PVC-PHPA, its correspondent homopolymers and the initiator iodoform. The copolymer demonstrates features of both of the homopolymers, as well as those of C-I bond active chain ends. The presence of the PHPA functional groups is shown by the broad band that corresponds to alcohol groups and ester groups. Carbon-chlorine bonds are not clearly shown in this spectrum due to the lower level of incorporation of PVC.

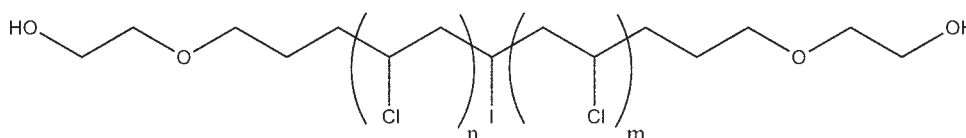


Figure 6 Chemical structure of PVC-OH²².

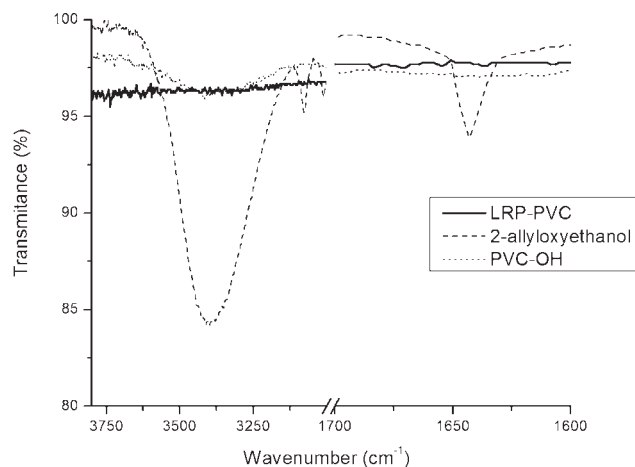


Figure 7 FTIR spectra of PVC-OH, LRP-PVC and 2-allyloxyethanol (hydroxyl and vinyl group regions).

For a better evaluation of the inclusion of the PVC segments (PHPA and PVC-PHPA being insoluble in commonly used solvents in NMR analysis), ^{13}C NMR solid state analysis was undertaken on samples PHPA and PVC-PHPA. The obtained spectra are presented in Figure 10. The presence of the PVC segment of PVC-PHPA becomes clearer from the presence of the peak at 58.7 ppm.³⁴ The other PVC group that should be around 47.4 ppm³⁴ is seemingly hidden by the PHPA methylene group peaks. The methyl group shows resonance signals between 20 ppm, and the methyleneoxy groups, from the two isomers of PHPA, show peaks between 63 and 73 ppm.³⁵ Carbonyl carbon atoms from PHPA can be identified in the region between 170 and 180 ppm.^{35,36} The active chain ends can be identified by the peak at around 17 ppm.³⁷ The reduction of the peak from PHPA to PVC-PHPA can be explained by the growth of the copolymer molecular weight through reaction of the former active chain ends with VCM. Chlorine microanalysis indicates a total PVC incorporation of 10.2 % (wt.) in the produced copolymer.

Melt mixing behaviour

Figure 11 shows the torque that is exerted by the blades during the melt mixing for products on different coupling agents and different compositions in the polymeric phase. To avoid PVC degradation, the

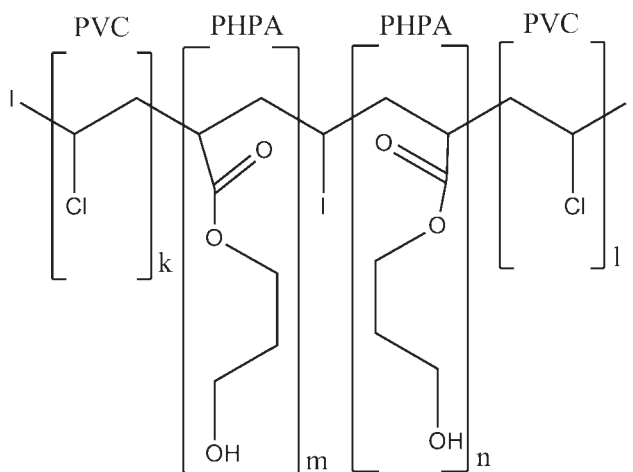


Figure 8 Chemical structure of PVC-PHPA.

mixing process was stopped at the first hint of material fusion.

The presence of wood flour strongly increases the torque of the mixture. PVC powders and wood flour are very different in respect of the particle shape and intermolecular forces. The increasing torque, when compared with that associated with the melting of PVC powders, is attributed to such differences. The inclusion of materials in the formulation, that can promote association between the PVC and the wood flour phases, leads to a decrease in the torque. This effect is greater when PVC-PHPA is used. Even for lower levels than that which is used with the other coupling agents, the effect of stabilising the mixture (leading to a lower torque) is enhanced with the increased PVC-PHPA content in the formulation. The presence of such a coupling agent allows for an increased degree of entanglement between the PVC and the wood flour. This leads to a less effort being required to promote their mixing.

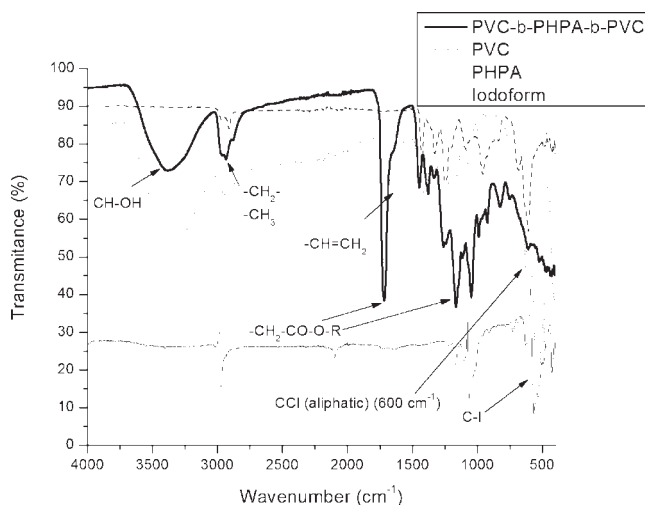


Figure 9 FTIR spectra of the PVC-PHPA, of the respective homopolymers and of the initiator, iodoform.

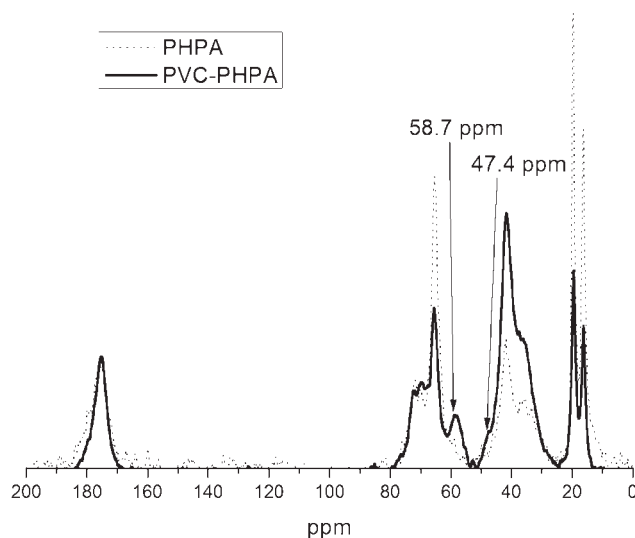


Figure 10 ^{13}C Solid state NMR spectra of PHPA and of PVC-PHPA.

Mechanical and thermal analysis

The mechanical and thermal characteristics were evaluated by DMA and by TGA. DMA is probably the most versatile thermal analysis method available. No other single test method providing more information from a single test.³⁸ In DMA, the material is subjected to a forced mechanical vibration at a fixed frequency, temperature, and elongation. A fraction of the energy is absorbed (E'' , viscous component) and a fraction is returned elastically (E' , elastic component). The determination of the ratio of these events enables clear evaluation of the mechanical performance. Other parameters may also be monitored, such as the miscibility between different compounds in the composite and any thermal events. DMA, in multifrequency analysis, allows one to distinguish between frequency dependent processes and those that are not. Molecular relaxations, such

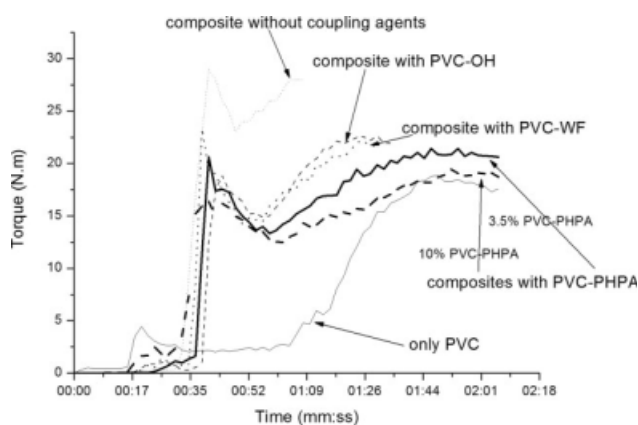


Figure 11 Torque exerted by the mixing of the materials in the fusion chamber, depending on the time and the coupling agents present in the formulation.

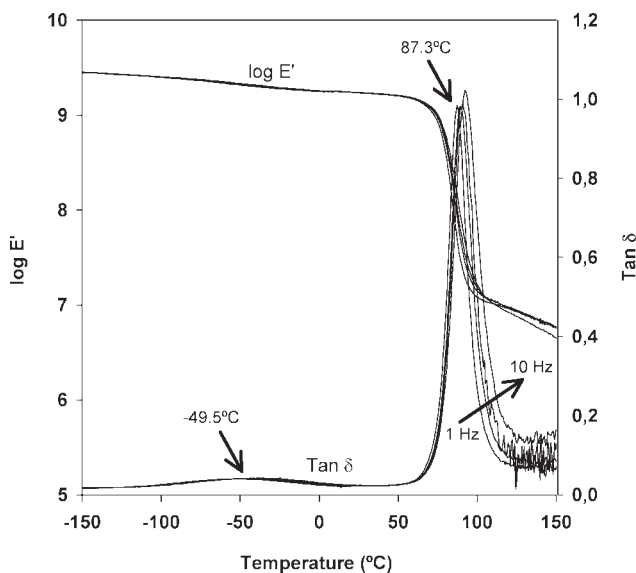


Figure 12 DMA of PVC (raw material).

as α relaxations (or glass transitions), β relaxations, and the peak of $\tan \delta$, are always frequency dependent.³⁷ Examples of processes that are not frequency dependent are melting, thermal degradation, curing and crystallization. Figure 12 shows the DMA thermograms of the PVC that was used in this work.

Figure 12 reveals β and α transitions of the PVC at -49.5°C and at 87.3°C , respectively. The $\tan \delta$ at 1 Hz and the TGA traces of the major raw-materials, PVC and wood flour, are compared in Figure 13.

Figure 13 reveals two major thermal transitions for the wood flour that was used in this work. The first transition is a broad peak in the DMA thermogram, between 10°C and 100°C , which can be related to the movement of chains that is associated to the

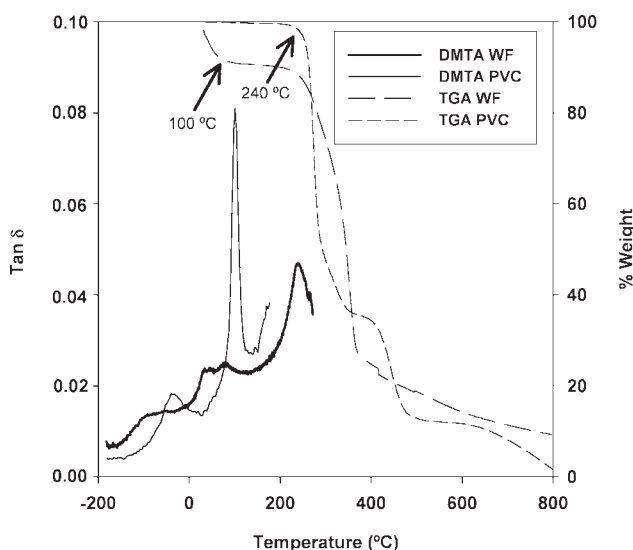


Figure 13 DMA (at 1Hz) and TGA traces of PVC (raw material) and wood flour.

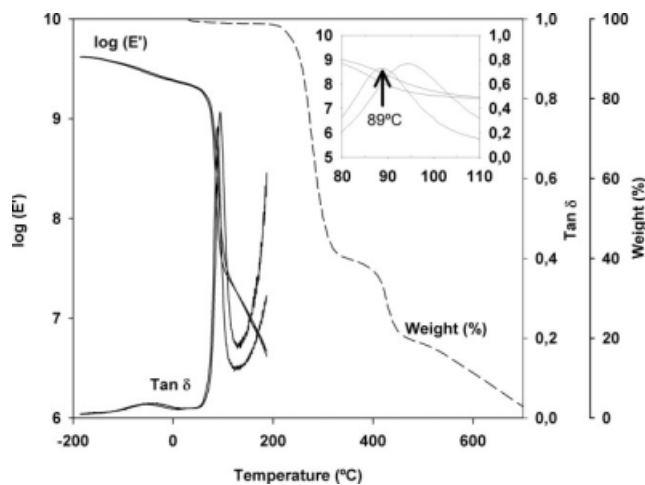


Figure 14 DMA (at 1Hz) and TGA traces of M01 (Table I).

presence of moisture. The TGA thermogram of the same sample shows that the first weight loss ends at 100°C . The second peak, at around 240°C , is associated with sample degradation and can be identified either by TGA or by DMA. Regarding the PVC sample, it is possible to observe frequency dependent transitions (in Fig. 13 these are represented only the $\tan \delta$ at 1 Hz) that correspond to the β and α transitions of the PVC, respectively.³² According to the degradation profile shown in Figure 13, the PVC and wood flour materials present higher degradation ratios only after 240°C .

Figure 14 illustrates the DMA and TGA traces for M01 (Table I). Sample M01 is the reference material, used for thermal analysis since it contains only the PVC and the wood flour.

The presented profile shows typical thermal behaviour for a plastic material. E' decreases nearly steadily with the temperature until the glass transition temperature (temperature at which the greatest decrease in E' occurs). The T_g , at 89°C , can be confirmed by the sensitivity of $\tan \delta$ at this temperature to the frequency of analysis. The $\tan \delta$ trace of M01 is close to that of the PVC materials, in terms of damping peaks (for shape and temperature values, see also Fig. 12). This suggests that the wood flour plays the role of filler in the composite, the PVC being responsible for the matrix of the composite. After the T_g , the composite presents no plateau of $\log E'$ and loses very quickly its elastic capacity. Rubbery flow occurs just after the T_g . At around 180°C , the composites become extremely soft and the single cantilever experiment ends. At this temperature, the matrix made of PVC loses its mechanical resistance, reaching the softening temperature of the PVC. In terms of the degradation profile the composite shows a similar pattern to that observed with PVC alone. It is interesting to note that the weight loss up to 100°C , for sample M01, is minimal

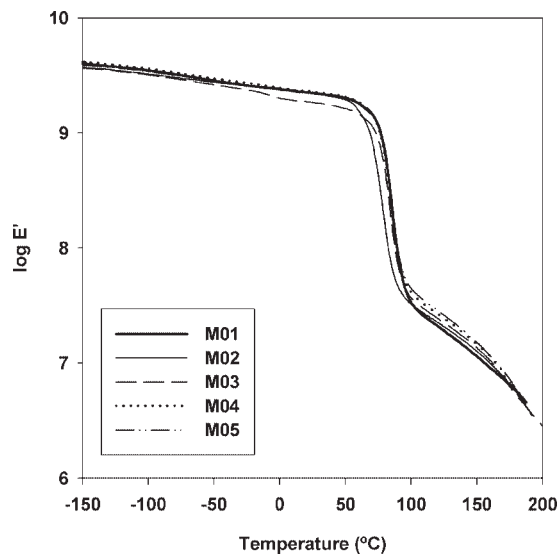


Figure 15 Elastic modulus of the different composites.

compared to the mass loss of the wood flour alone. The cause of this effect is the high processing temperature that eliminates the wood flour moisture.

The elastic modulus of the different composites is presented in Figure 15. The results suggest that the different composites present the same mechanical behaviour within the range of the testing temperatures. The different samples show a consistent decrease in the elastic modulus with temperature increase until around 50°C. After this, a sharp decrease occurs. This indicates the beginning of the movement of the main chains.

A closer view of the traces over very low temperatures is presented in Figure 16, showing clearly the relative values of the E' for the different composites at these lower temperatures.

The results show that the amount of VC-PHPA that is added can have dissimilar effects on the elastic modulus. The addition of 3.5% to the formulation creates a higher elastic modulus in the composite, whereas the addition of 10% creates a lower elastic modulus. Increasing the amount of PVC-PHPA can lead to such a degree of association between the PHPA molecules that the elastic properties of the material become poorer. In spite of the dissimilar behaviour described above, it is interesting to notice that, at -20 °C, the elastic modulus of the majority of the samples is similar. The only samples that fall outside this trend are the samples to which the copolymer of PVC-PHPA was added. The mechanical properties of the composites, with increasing temperature, are affected by the presence of the wood flour and the coupling agents, leading to slight differences in the values of E' for each temperature. The influence of PVC-OH and PVC-WF, used as coupling agents, is less pronounced compared with their influence on the composites produced using

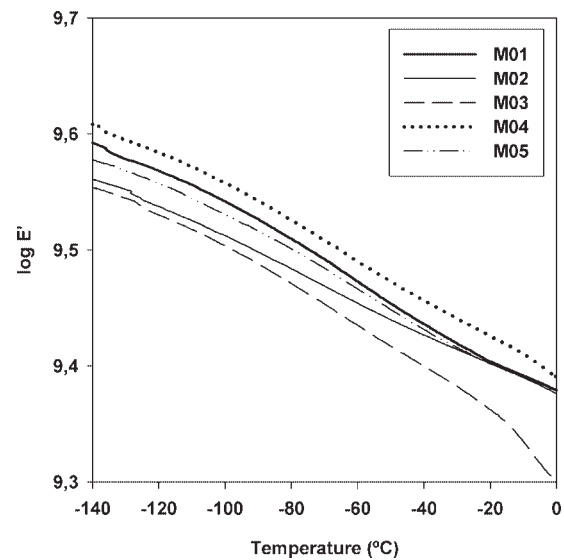


Figure 16 Elastic modulus of the different composites below 0°C.

PVC-PHPA. Functionalised PVC-OH and PVC-WF, when used as coupling agents in the composite PVC/wood flour, did not introduce major differences in the composites. However, considering the results obtained, the addition of the copolymer PVC-b-PHPA-b-PVC may be a matter of optimisation, in terms of mixing and composition, to achieve the desired performance properties.

The E'' obtained for the composites is presented in Figure 17. Here it is possible to verify that the composite with the lower viscosity is the reference, prepared with only PVC and wood flour, confirming the success in the enhancement of the association between the PVC and wood flour, when the coupling agents were added. It is interesting to note

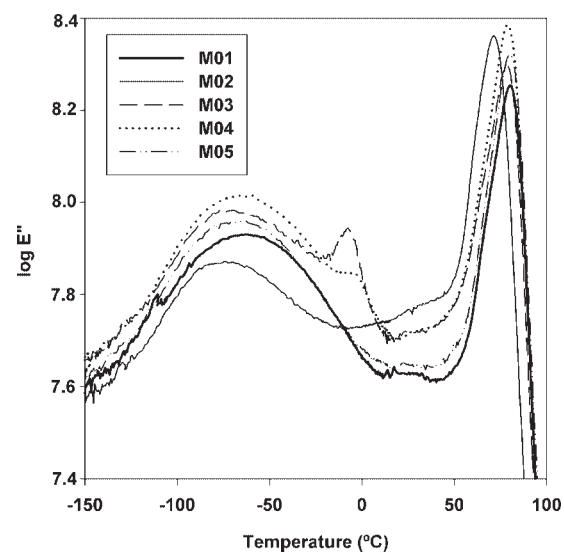


Figure 17 Loss modulus of the different composites at 1 Hz.

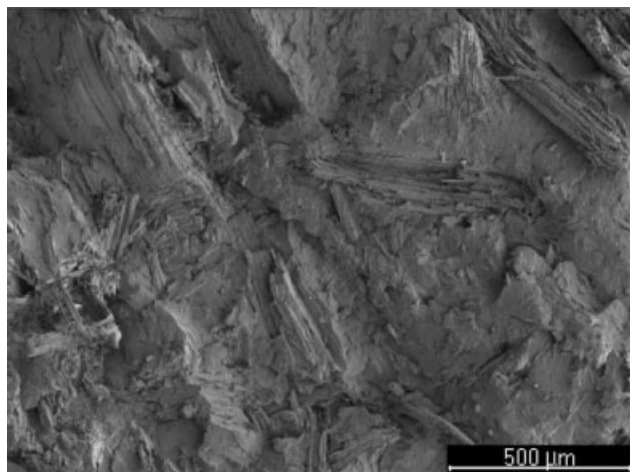


Figure 18 SEM electron micrograph of sample M01 (Mag. $\times 70$).

that the composite M04 (Table I) is the sample that presents the higher viscosity and elastic modulus. This result suggests the presence of increasing entanglement between the PVC and the wood flour.

Figures 18 and 19 show SEM electron micrographs of a composite that was formulated without coupling agents (M01) and one formulated with 3.5% of PVC-PHPA (M04). For M01, it is possible to observe clearly the defined forms of the wood flour. However, for sample M04, because of the coupling agent, and, in agreement with the DMA results, the compatibility between the wood flour and the PVC matrix is increased. Thus, in Figure 19 it is no longer possible to distinguish clearly the full wood flour particles, due to a better entanglement with the PVC matrix.

M02 (Table I) shows a profile that is slightly different from what was expected, considering that the elastic modulus results did not show major differen-

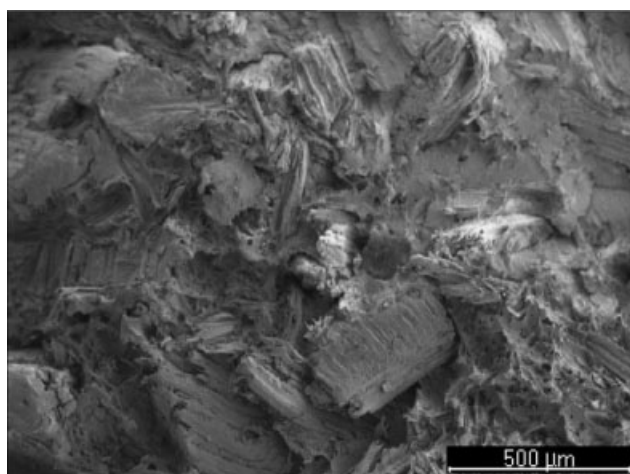


Figure 19 SEM electron micrograph of sample M04 (Mag. $\times 70$).

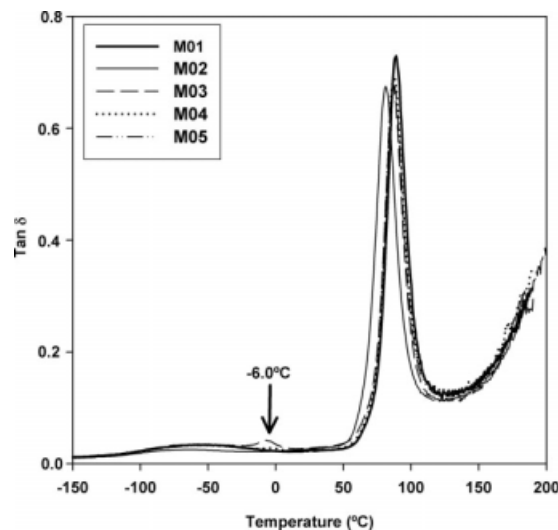


Figure 20 Tan δ of the different composites.

ces from the results for M01. Two possible explanations can be given to this profile. One concerns the plasticising effect created by the inclusion of hydroxyl groups at the LRP-PVC chain ends. The second concerns small amounts of the possible remaining reaction solvent. However, it should be noted that the product was washed and dialysed several times before thorough drying to constant mass.

Figure 20 presents the damping effect for the different composites that were prepared for this work. The results indicate that the T_g is only slightly affected over the different formulations studied. The only exception arises with sample M02 which has a lower T_g than that of the other samples. The presence of the small peak at -6.0°C should be noted.

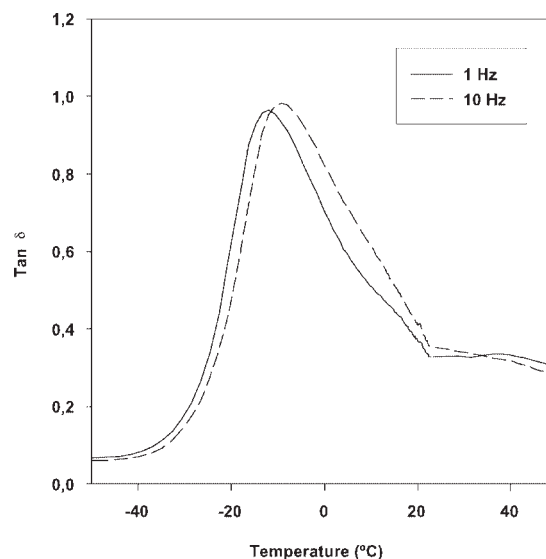


Figure 21 Tan δ of the block copolymer PVC-b-PHPA-b-PVC.

TABLE II
Mechanical and Thermal Properties of the Composites

Sample	E' (GPa)		E' (GPa)		T _g (°C)	ΔH (kJ/mol)
	-50°C	0°C	-50°C	0°C		
PVC	2.10	1.80	82	46	87.3	242.5
M01	2.86	2.38	82	46	89.0	210.6
M02	2.76	2.36	71	53	81.1	11.5
M03	2.60	2.00	89	70	86.5	188.3
M04	3.00	2.45	120	71	87.0	209.0
M05	2.88	2.39	87	48	87.6	212.5

Figure 21 represents the DMA plot of the block copolymer PVC-b-PHPA-b-PVC, that was used to formulate the composites M03 and M04 (Table I). From Figure 21 it is possible to identify the small peak at -6.0 °C as being the T_g for the block copolymer. The presence of this peak in the DMA trace of the composites M03 and M04 indicates some immiscibility of PVC-PHPA. However, the immiscibility issue does not account for the increase of E' for the composite M04, as seen in Figure 21. One possible reason for the presence of the immiscibility could be the very high proportion of PHPA relative to the PVC in the copolymer (around 9 : 1 in weight). This leads to a copolymer that is rich in PHPA and with a greater tendency to stick together, causing phase segregation during the processing.

The different composites present a small peak that is sensitive to the applied frequency at temperatures around -50°C. This corresponds to the β transition of PVC that did not disappear, regardless of the formulation used, confirming the high dependence on the PVC matrix.

Table II summarises the major mechanical and thermal parameters for the different composites studied.

The composite M01 presents the lower values of E' compared with those for the other composites. The enhancement of the elastic modulus that was observed for the other composites of PVC/wood flour can be attributed to greater association between the wood flour and the polymeric matrix, in this case the PVC. The presence of these coupling agents makes possible a real reinforcement of the PVC matrix with the wood flour. This increase in interfacial association, and in the degree of reinforcement, could also restrict the free motion of the PVC chain matrix, leading to an increased viscosity and a corresponding increase in the loss of modulus,¹¹ as observed in the E'' values. The glass transition temperatures are slightly affected, but the presence of the coupling agents seems to give a plasticising effect to the product relative to the flexibility that is shown by the PVC/wood flour formulation without the coupling agents. In terms of the energy involved in the glass transition process, the values are in the

same range. However, the increasing complexity of the system seems to cause a moderate decrease in these energies. Again, M02 presents values that are completely different.

To validate the consistent results obtained from the DMA analysis, composites containing 50% of Bubinga wood flour together with 0, 5, and 10% by weight of PVC-b-PHPA-b-PVC were submitted for flexural experiments. The strengths at yield point were 91.7 ± 4.7 , 103 ± 1.0 , and 77.5 ± 5.8 MPa, respectively. These results are in agreement with the trends shown in DMA results, indicating improved mechanical properties for samples with small amounts of PVC-b-PHPA-b-PVC and then a decrease in the strength of the composite as this amount increases.

CONCLUSIONS

The results presented suggest the possibility for improving the mechanical properties of PVC/wood flour composites by adding components that were prepared using a living radical polymerisation method. These materials improve the melt mixing process, leading to a lower stress being applied during the mixing. The block copolymer PVC-b-PHPA-b-PVC is the coupling agent that gave the best results, leading to a mixing process for the PVC and the wood flour that is similar to that of the PVC alone. This block copolymer, at certain loadings, enhanced the mechanical properties of the PVC/wood flour composites. However, for higher loadings phase separation, due to increased association between PHPA molecules, can occur leading to poorer mechanical properties. The results showed the improved reinforcement of the PVC matrix by the wood flour, when coupling agents, of the type described, are used.

References

1. Jain, R. K.; Singh, Y.; Rai, M. *Building Environ* 1977, 12, 277.
2. Stokke, D. D.; Gardner, D. J. *J Vinyl Additive Technol* 2003, 9, 96.
3. Jiang, H.; Kamdem, D. P. *J Vinyl Additive Technol* 2004, 10, 59.

4. Wood filled plastics: the time has come! *Plastics Engineering* 2005.
5. Kosonen, M. L.; Wang, B.; Caneba, G. T.; Gardner, D. J.; Rials, G. *Clean Prod Processes* 2000, 2, 117.
6. Li, T. Q.; Wolcott, M. P. *Compos Part A: Appl Sci Manufacturing* 2004, 35, 303.
7. Devi, R. R.; Maji, T. K.; Banerjee, A. N. *J Appl Polym Sci* 2004, 93, 1938.
8. Baysal, E.; Ozaki, S. K.; Yalinkilic, M. *Wood Sci Technol* 2004, 38, 405.
9. Georgopoulos, S. T.; Tarantili, P.; Avgerinos, E.; Andreopoulos, A.; Koukios, E. *Polym Degrad Stab* 2005, 90, 303.
10. Jiang, H.; Kamdem, D. P. *J Vinyl Additive Technol* 2004, 10, 70.
11. Shah, B. L.; Matuana, L. M.; Heiden, P. A. *J Vinyl Additive Technol* 2005, 11, 160.
12. Kim, J.; Peck, J. H.; Hwang, S.; Hong, J.; Hong, S. C.; Huh, W.; Lee, S. *J Appl Polym Sci* 2008, 108, 2654.
13. Zhao, Y.; Wang, K.; Zhu, F.; Xue, P.; Jia, M. *Polym Degrad Stab* 2006, 91, 2874.
14. Pickering, K. L.; Abdalla, A.; Ji, C.; McDonald, A. G.; Franich, R. A. *Compos Part A: Appl Sci Manufacturing* 2003, 34, 915.
15. Valadez-Gonzalez, A.; Cervantes-Uc, J. M.; Olayo, R.; Herrera-Franco, P. J. *Compos Part B: Eng* 1999, 30, 321.
16. Torry, S.; Campbell, A.; Cunliffe, A.; Tod, D. *Int J Adhes Adhesives* 2006, 26, 40.
17. Wen, J.; Wilkes, G. L. *Polym Bull* 1996, 37, 51.
18. Bengtsson, M.; Oksman, K. *Compos Sci Technol* 2006, 66, 2177.
19. Kuan, C.-F.; Ma, C.-C. M.; Kuan, H.-C.; Wu, H.-L.; Liao, Y.-M. *Compos Sci Technol* 2006, 66, 2231.
20. Percec, V.; Popov, A. V.; Ramirez-Castillo, E.; Weichold, O. *J Polym Sci Part A: Polym Chem* 2003, 41, 3283.
21. Percec, V.; Popov, A. V.; Ramirez-Castillo, E.; Coelho, J. F. J.; Hinojosa-Falcon, L. A. *J Polym Sci Part A: Polym Chem* 2004, 42, 6267.
22. Percec, V.; Popov, A. V.; Ramirez-Castillo, E.; Coelho, J. F. J. *J Polym Sci Part A: Polym Chem* 2005, 43, 773.
23. Percec, V.; Popov, A. V. *J Polym Sci Part A: Polym Chem* 2005, 43, 1255.
24. Qiu, J.; Charleux, B.; Matyjaszewski, K. *Prog Polym Sci* 2001, 26, 2083.
25. Bledzki, A. K.; Faruk, O. *Compos Part A: Appl Sci Manufacturing* 2006, 37, 1358.
26. Kuan, C.-F.; Kuan, H.-C.; Ma, C.-C. M.; Huang, C.-M. *Compos Part A: Appl Sci Manufacturing* 2006, 37, 1696.
27. Sailaja, R. *Compos Sci Technol* 2006, 66, 2039.
28. Coelho, J. F. J.; Silva, A. M. F. P.; Popov, A. V.; Percec, V.; Abreu, M. V.; Gonçalves, P. M. O. F.; Gil, M. H. *J Polym Sci Part A: Polym Chem* 2006, 44, 2809.
29. Coelho, J. F. J.; Silva, A. M. F. P.; Popov, A. V.; Percec, V.; Abreu, M. V.; Gonçalves, P. M. O. F.; Gil, M. H. *J Polym Sci Part A: Polym Chem* 2006, 44, 3001.
30. Coelho, J. F.; Carreira, M.; Popov, A. V.; Gonçalves, P. M.; Gil, M. *Eur Polym J* 2006, 42, 2313.
31. Coelho, J. F.; Carreira, M.; Gonçalves, P. M.; Popov, A. V.; Gil, M. H. *J Vinyl Additive Technol* 2006, 12, 156.
32. Coelho, J. F. J. *New Technologies for Homopolymerization and Copolymerization of Vinyl Chloride*, Ph.D. Thesis, University of Coimbra, 2006.
33. Britcher, L. G.; Kehoe, D. C.; Matisons, J. G.; Swincer, A. G. *Macromolecules* 1995, 28, 3110.
34. Tavares, M. I. B.; Monteiro, E. E. C. *Polym Test* 1995, 14, 273.
35. Prasath, R. A.; Nanjundan, S.; Pakula, T.; Klapper, M. *J Appl Polym Sci* 2006, 100, 1720.
36. Hervé, M.; Hirschinger, J.; Granger, P.; Gilard, P.; Deflandre, A.; Goetz, N. *Biochim Biophys Acta* 1994, 1204, 19.
37. Wilberg, K. B.; Pratt, W. E.; Bailey, W. F. *J Org Chem* 1980, 45, 4936.
38. Menard, K. P. *Dynamic Mechanical Analysis - A Practical Introduction*, 1st ed.; CRC Press: London, 1999.